Title

In Vivo Fate of Cowpea Mosaic Virus In Situ Vaccine: Biodistribution and Clearance

Journal

ACS Nano, 16(11)

ISSN

1936-0851

Authors

de Oliveira, Jessica Fernanda Affonso
Chan, Soo Khim
Omole, Anthony O
et al.

Publication Date

2022-11-22

DOI

10.1021/acsnano.2c06143

Peer reviewed

HHS Public Access

Author manuscript

ACS Nano. Author manuscript; available in PMC 2023 January 14.

Published in final edited form as:

ACS Nano. 2022 November 22; 16(11): 18315–18328. doi:10.1021/acsnano.2c06143.

In Vivo Fate of Cowpea Mosaic Virus In Situ Vaccine: Biodistribution and Clearance

Jessica Fernanda Affonso de Oliveira[¶],
Department of NanoEngineering, University of California San Diego, La Jolla, California 92039, United States

Soo Khim Chan[¶],
Department of NanoEngineering, University of California San Diego, La Jolla, California 92039, United States

Anthony O. Omole,
Department of NanoEngineering, University of California San Diego, La Jolla, California 92039, United States

Vanshika Agrawal,
Department of NanoEngineering, University of California San Diego, La Jolla, California 92039, United States

Nicole F. Steinmetz
Department of NanoEngineering, University of California San Diego, La Jolla, California 92039, United States; Center for Nano-ImmunoEngineering, Department of Bioengineering, Department of Radiology, Moores Cancer Center, and Institute for Materials Discovery and Design, University of California San Diego, La Jolla, California 92039

Abstract

Cowpea mosaic virus (CPMV) is a nucleoprotein nanoparticle that functions as a highly potent immunomodulator when administered intratumorally and is used as an in situ vaccine. CPMV in situ vaccination remodels the tumor microenvironment and primes a highly potent, systemic, and durable antitumor immune response against the treated and untreated, distant metastatic sites (abscopal effect). Potent efficacy was demonstrated in multiple tumor mouse models and, most importantly, in canine cancer patients with spontaneous tumors. Data indicate that presence of anti-CPMV antibodies are not neutralizing and that in fact opsonization leads to enhanced efficacy.

Corresponding Author Nicole F. Steinmetz – Department of NanoEngineering, University of California San Diego, La Jolla, California 92039, United States; Center for Nano-ImmunoEngineering, Department of Bioengineering, Department of Radiology, Moores Cancer Center, and Institute for Materials Discovery and Design, University of California San Diego, La Jolla, California 92039, United States; nsteinmetz@ucsd.edu.

[¶]Author Contributions
J.F.A.dO. and S.K.C. contributed equally.

Supporting Information
The Supporting Information is available free of charge at https://pubs.acs.org/doi/10.1021/acsnano.2c06143.
Detailed experimental procedures and supporting data for CPMV stability under simulated gastric and intestinal fluid as well as additional biodistribution data and photographs of plants (PDF)

The authors declare the following competing financial interest(s): Dr. Steinmetz is a co-founder of, has equity in, and has a financial interest with Mosaic ImmunoEngineering Inc. Dr. Steinmetz serves as Director, Board Member, and Acting Chief Scientific Officer, and paid consultant to Mosaic. The other authors declare no potential conflict of interest.

Plant viruses are part of the food chain, but to date, there is no information on human exposure to CPMV. Therefore, patient sera were tested for the presence of immunoglobulins against CPMV, and indeed, >50% of deidentified patient samples tested positive for CPMV antibodies. To get a broader sense of plant virus exposure and immunogenicity in humans, we also tested sera for antibodies against tobacco mosaic virus (>90% patients tested positive), potato virus X (<20% patients tested positive), and cowpea chlorotic mottle virus (no antibodies were detected). Further, patient sera were analyzed for the presence of antibodies against the coliphage Qβ, a platform technology currently undergoing clinical trials for in situ vaccination; we found that 60% of patients present with anti-Qβ antibodies. Thus, data indicate human exposure to CPMV and other plant viruses and phages. Next, we thought to address agronomical safety; i.e., we examined the fate of CPMV after intratumoral treatment and oral gavage (to mimic consumption by food). Because live CPMV is used, an important question is whether there is any evidence of shedding of infectious particles from mice or patients. CPMV is noninfectious toward mammals; however, it is infectious toward plants including black-eyed peas and other legumes. Biodistribution data in tumor-bearing and healthy mice indicate little leaching from tumors and clearance via the reticuloendothelial system followed by biliary excretion. While there was evidence of shedding of RNA in stool, there was no evidence of infectious particles when plants were challenged with stool extracts, thus indicating agronomical safety. Together these data aid the translational development of CPMV as a drug candidate for cancer immunotherapy.

Graphical Abstract

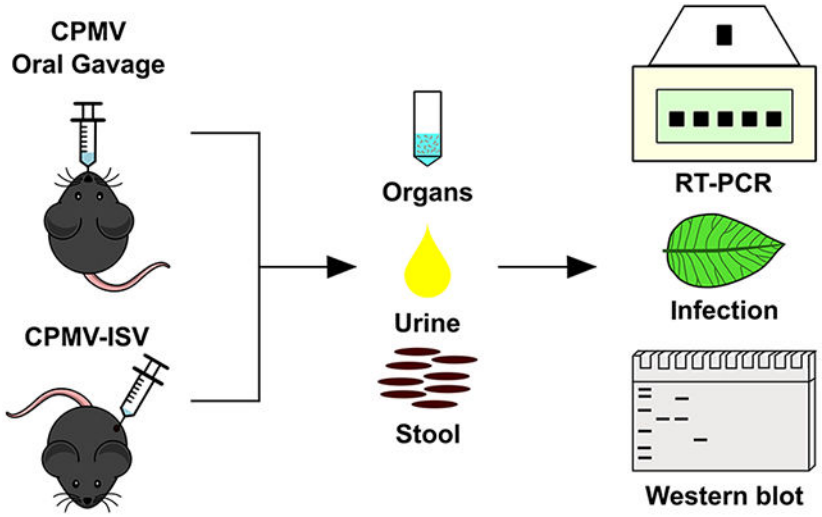

Keywords

cowpea mosaic virus; in situ vaccine; translational research; biodistribution; clearance; shedding

INTRODUCTION

Several nanoparticle formulations have progressed through clinical development and are now approved for use in humans or companion animals.[1,2] Each formulation, viral or synthetic, has their advantages and properties to be utilized in nanomedicine.[3] Our interests

lie in the development of plant viral nanoparticles (VNPs) and virus-like particles (VLPs) that can be manufactured at high yields through plant molecular farming or fermentation.[4-7] The diversity of plant viruses offers a library of biological materials with different structures to choose from, including icosahedrons, nanotubes, or filamentous structures (typically <500 nm in size).[8-11] Their structural properties lend them as templates for chemical and synthetic engineering such as shape-tuning, encapsulation or infusion, bioconjugation, or genetic tailoring with cargos ranging from small molecules to proteins and even synthetic nanoparticles.[12-15] VNPs and their noninfectious counterparts, the VLPs, also offer a high degree of structural uniformity, quality control, and assurance, as they yield monodispersed nanoparticles.[16]

Mammalian viruses have been established for use in gene therapy and immunotherapy, with some vaccines being produced using inactivated viruses or VLPs.[17-20] Examples include vaccines against hepatitis B virus (Sci-B-Vac) and human papilloma virus (Cervarix, Gardasil, and Gardasil9).[21,22] More recent formulations use plant viruses and VLPs from bacteriophages, for example, Checkmate Pharmaceuticals' Vidutolimod (formerly known as CMP-001, CYT003, or QbG10), which is a CpG-A-loaded Qβ VLP used as a cancer immunotherapeutic.[23,24] Relevant to COVID-19, plant-based vaccines have also emerged as an attractive alternative to rapidly produce COVID-19 vaccines through molecular farming. Among some companies, Medicago developed the CoVLP vaccine candidate—a VLP expressed in plant tissue—while US-based Kentucky BioProcessing (KBP) developed the KBP-201 vaccine candidate based on tobacco mosaic virus (TMV) displaying the SARS-CoV-2 RBD domain.[25]

Our laboratory is developing a plant-virus-based in situ vaccine (ISV) with demonstrated efficacy in multiple tumor mouse models and canine patients. Specifically, cowpea mosaic virus (CPMV)[26-30] is used, and we capitalize on the immunostimulatory nature of the plant virus that when injected intratumorally (I.T.) activates innate immune cells within the tumor microenvironment (TME), therefore overcoming the immunosuppressive features of cold and aggressive tumors. The potency of CPMV as an ISV has been demonstrated in multiple tumor mouse models and canine cancer patients; abscopal effect and long-lasting protection from rechallenge or recurrence of the disease was documented.[31-34]

CPMV, a plant virus in the Secoviridae family, measures 30 nm in diameter and consists of 60 copies each of large (L) and small (S) coat protein subunits.[35] In previous research, we considered CPMV, genome-free CPMV (termed empty CPMV or eCPMV[36]), as well as UV-inactivated CPMV[33,34,37,38] and determined that the wild-type CPMV is the most potent ISV formulation. eCPMV-ISV being the least potent of the three formulations still demonstrates high antitumor potency in mouse models and canine patients;[30-32] however, direct comparison with chemically inactivated CPMV or native CPMV highlights the importance of the nucleic acid cargo for immune cell signaling through Toll-like receptor (TLR)-7.[33,38] Mechanism of action studies revealed that CPMV primes innate immune activation through MyD88-dependent pathways and signals through TLR-2, −4, and −7.[33] UV-inactivated CPMV (with heavily cross-linked RNA and protein components) and eCPMV do not signal through TLR-7 and therefore lack type I interferons, which may be

a critical stimulation in potentiating antitumor immunity.[33,37] For these reasons, we propose native, live CPMV for translational development.

Although wild-type CPMV is not known to be infectious to humans or mammals, it infects plants, including black-eyed peas and other legumes.[39,40] Currently, it is estimated that around 1000 plant viruses are known[41] which cause negative impacts on crop production, food security, and ultimately cause an economic burden.[42-44] It is also known that there is human exposure to plant viruses. Some plant viruses are commonly found in the human gut virome (tobacco mosaic virus, TMV; pepper mild mottle virus, PMMoV; tomato mosaic virus, ToMV),[45-48] and there are reports of shedding of plant viruses from humans.[48] For the translational development of live CPMV as a drug candidate, it is important to understand human exposure and potential shedding of infectious particles to determine agronomical safety.

To the best of our knowledge, there are no reports investigating human exposure to CPMV. Therefore, our first aim was to probe whether humans are exposed to CPMV. We analyzed human plasma from a 50 patient cohort for the presence of anti-CPMV antibodies. We also considered TMV, potato virus X (PVX), cowpea chlorotic mottle virus (CCMV), and the bacteriophage Qβ to obtain broader insights into plant virus and phage human exposure. Our second aim was to investigate the biodistribution and clearance of CPMV in healthy and tumor-bearing mice (a murine melanoma model was used) when administered orally or intratumorally. Specifically, we considered whether infectious particles were shed in urine or stool.

RESULTS AND DISCUSSION

CPMV and Cy5-CPMV Synthesis and Characterization.

Native and fluorescently labeled Cy5-CPMV was prepared, and the latter was used for particle trafficking studies. Cy5-CPMV was synthesized by conjugating N-hydroxysuccinimide (NHS) ester of sulfo-Cy5 (NHS-Sulfo-Cy5) to CPMV's solvent-exposed lysine residues.[49] CPMV and Cy5-CPMV were characterized to confirm the degree of labeling, purity, and particle integrity (Figure 1). Native and denaturing gel electrophoresis was consistent with the presence of intact CPMV and Cy5-CPMV particles, and protein contaminants or free dye were not apparent. Native gels of intact particles showed cocolocalization of RNA and protein components and, in the case of Cy5-CPMV, also fluorescence (Figure 1B). Denaturing sodium dodecyl sulfate polyacrylamide gel electrophoresis (SDS-PAGE) (Figure 1C) showed the ~24 kDa (S) and ~42 kDa (L) coat protein subunits for CPMV and fluorescently labeled coat proteins of Cy5-CPMV. The degree of labeling was determined by UV–vis (Figure 1D), revealing labeling with ~40 Cy5 dyes per CPMV.

Particle integrity was determined using size exclusion chromatography (SEC, Figure 1E), transmission electron microscopy (TEM, Figure 1F), and dynamic light scattering (DLS, Figure 1G). Both CPMV and Cy5-CPMV showed similar elution profiles and eluted at 10–15 mL from a Superose 6 increase column with the characteristic 260/280 ratio of ~1.8.[50] TEM imaging depicts monodisperse ~30 nm sized particles; data were corroborated by

DLS measurements, which indicated a hydrodynamic diameter of CPMV and Cy5-CPMV measuring ~35 nm with a narrow polydispersity index (PDI) of 0.1.

Prevalence of Anti-VNP/VLP Antibodies in Humans.

We searched viral databases developed by the University of Georgia's Center for Invasive Species and Ecosystem Health (https://www.prevalentviruses.org/index.html) and the Center for Agriculture and Bioscience International (CABI, https://www.cabi.org/what-we-do/invasive-species/) for the global and U.S. distribution of CPMV and other plant viruses (TMV, CCMV, and PVX). From this, TMV is the most prevalent plant virus with distribution throughout the U.S. and globally (Figure 2).[46,51] PVX also showed a broad U.S. and global distribution—it is found in places where potatoes are produced and traded.[52] CPMV and CCMV, both of which infect legumes including black-eyed peas, have narrow distribution; principally, they are found in Nigeria, Uganda, and some states in the U.S., such as Missouri, Texas, and Michigan (Figure 2B).[53] A common insect vector for bean-infecting viruses is the *Ceratoma trifurcata* beetle,[54] and this is commonly found around the Mississippi Delta and in Ontario, Canada (which shares a border with Michigan).[55] CPMV and CCMV appear to be prevalent in the regions where *C. Trifurcata* is found.[55]

To assess human exposure to CPMV and other plant viruses, we tested a cohort of 50 deidentified patients for the presence of antibodies against CPMV, TMV, PVX, and CCMV; we also included VLPs from bacteriophage Qβ (Figure 3). Under-standing prevalence of antiviral antibodies in humans provides insights into human exposure of different plant viruses and their immunogenicity. This is of importance for the translation of CPMV into clinical trials as the presence of anti-CPMV antibodies may impact the clinical dosing strategy. For CPMV-ISV, antibody opsonization does not limit efficacy but instead boosts it: antibody opsonization of CPMV results in more rapid uptake by innate immune cells, which are the target cell population, and data indicate that animals preimmunized against CPMV with confirmed anti-CPMV titers exhibit enhanced antitumor potency compared to CPMV-ISV using naïve tumor-bearing animals.[27,50] This phenomenon also holds true in the CpG-laden Qβ-ISV platform.[23] In fact, here, because Qβ does not interact efficiently with innate immune cells, patients are first vaccinated against Qβ; only after establishment of anti-Qβ immunity is ISV treatment performed. However, it should be noted that CPMV, in stark contrast to Qβ, efficiently targets and is taken up by innate immune cells even in the absence of opsonizing antibodies. Nevertheless, understanding the prevalence of anti-CPMV antibodies in humans is important to gain an understanding of plant virus exposure and may help define clinical protocols for CPMV-ISV.

CCMV was included in the study due to its similar distribution compared to that of CPMV. It also shares structural similarity in that is forms 30 nm sized icosahedrons packaging a multipartite RNA genome[27] but is generally less stable when compared to CPMV. We included TMV in this study because of its wide distribution globally, and because anti-TMV antibodies have been documented in humans,[46,51] TMV served as a positive control. To test another example of a plant virus with broader global distribution but unknown human exposure, we also considered the filamentous PVX.[58,59]

Patients' plasma samples were obtained from UC San Diego's Research Biobank and screened for anti-VNP/VLP antibodies using enzyme-linked immunosorbent assay (ELISA). In this cohort, 52% of patients presented anti-CPMV antibodies with titers in varying degrees, which may be attributed to dietary differences.[60] As expected,[46,51] 92% of patients presented anti-TMV antibodies. Interestingly, CCMV antibodies were not detected in the patient cohort, and only 18% of patients presented anti-PVX antibodies, which is in contrast with the global distribution of PVX. We hypothesize that prevalence of antiplant virus antibodies is a combination of distribution and exposure through food but also a result of particle stability—antibodies are prevalent for TMV and CPMV, which are the more stable nanoparticle formulations compared to PVX and CCMV. While TMV and CPMV are known to be stable under a wide range of pH, resistant to various solvents and temperature,[39,61-63] CCMV undergoes pH- and salt-dependent disassembly,[64] and the PVX coat protein is sensitive to proteolysis by the digestive enzymes presented at the gastrointestinal tract (GI).[65] Decreased stability may lead to degradation after oral uptake, therefore preventing bioavailability and development of immune responses against the particle. Lastly, 60% of the patient cohort also tested positive for anti-Qβ antibodies. Qβ is a coliphage and thus infects *Escherichia coli* present in the gut of humans and other mammals; this may explain Qβ exposure.[66] To conclude, these findings indicate that humans are exposed to CPMV and that anti-CPMV antibodies are prevalent.

Immunogenicity of CPMV in Mice.

Previous research using a mouse model of intraperitoneal (I.P.) disseminated ovarian cancer indicates that anti-CPMV antibodies are produced over the course of ISV treatment (six weekly doses of 100 μg of CPMV).[50] Here, we determined whether antibodies are also produced after CPMV-ISV using a dermal melanoma model. Further, because we found that anti-CPMV antibodies are prevalent in humans (see Figure 3), we also tested the immunogenicity of the CPMV after oral gavage (O.G.) administration. Healthy and B16F10 dermal melanoma-bearing mice received three doses (O.G. or I.T.) of CPMV or Cy5-CPMV, 5 days apart (100 μg/20 μL phosphate-buffered saline (PBS) for I.T. and 100 μg/300 μL PBS for O.G.), to mimic consumption through feeding or the CPMV-ISV schedule for treatment of dermal melanoma, respectively. Sera were collected and analyzed for anti-CPMV antibodies using ELISA (Figure 4).

CPMV and Cy5-CPMV are highly immunogenic, with end point titers that reach 1:800 after a single I.T. dose, 1:204,800 after the second I.T. dose, and 1:819,200 after the third I.T. dose (Figure 4A). While comparable titers were observed after prime-boost for the O.G. group (Figure 4B,C), repeated dosing was needed to detect any antibodies; this may be explained by the delayed processing time of the samples when subjected to the oral route. Overall data are consistent and expected; CPMV is immunogenic, and antibodies against the plant virus are produced independently of the administration route.

Biodistribution and Clearance of CPMV.

CPMV in vivo trafficking was evaluated using CPMV and Cy5-CPMV particles in tumor-bearing (B16F10 melanoma) and healthy C57BL/6 mice. Mice received three doses of 100 μg of CPMV either I.T. or orally. This dose was chosen based on our standard dosing

scheme used for mouse model studies and canine patient treatment. The typical dose used for canine patients is 0.2 mg of CPMV; for example, a beagle presenting with a 5 cm large oral melanoma was treated using four injections of 0.2 mg of CPMV, administered I.T. over a 14 day treatment window.[30] A beagle weighs ~20 kg, hence the treatment dose was 0.1 mg/kg of CPMV, and we anticipate a similar dose for human clinical trials. In the present study, we used 5 mg/kg (0.1 mg per mouse), which is a 50-fold excess compared to the projected clinical dose and thus expected to provide insights into the biodistribution and clearance. Oral administration was included because data indicate the prevalence of anti-CPMV antibodies in humans, likely through exposure through the food chain. To assay for bioaccumulation and organ distribution, live animal imaging was performed (Figures 5); then organs and tumors were excised 24 h after the final treatment, and homogenized tissues were analyzed by fluorescence measurements (if treated with Cy5-CPMV, Figure 6A) and reverse transcription quantitative polymerase chain reaction (RT-qPCR) (Figure 6B,C).

Live animal imaging and fluorescence measurements indicate minimal accumulation in organs independent of the administration route—most interesting is the observation that I.T.-dosed CPMV persists within the tumor with minimal to no apparent leaching and systemic exposure (Figures 5 and 6A). We observed in previous studies that CPMV has good tumor retention properties, and mouse studies demonstrated that CPMV could be detected for up to 4 days post-I.T. administration in dermal melanoma,[67] up to 7 days post-administration in I.P. disseminated ovarian tumors,[68] and up to 5 days in orthotopic glioma.[29] The nanoparticle nature of CPMV likely prevents leaching and clearance from tumor tissue—in stark contrast, this presents a challenge for topical and I.T. administered small molecule therapeutics,[69] which also is clearly seen here—Cy5 is rapidly cleared from the tumors, but Cy5-CPMV persists for at least 5 days (Figure 5). Retention may be mediated simply by the nanoparticle size and hence slow tissue diffusion rate, phagocytosis by innate immune cells, and/or be in part mediated by CPMV's affinity to bind to surface-expressed vimentin found in various tumors.[27,70]

Next, RT-qPCR was used to further analyze the biodistribution profiles by probing for CPMV RNA-2, which encodes the CPMV coat proteins.[71,72] A standard curve was used to quantify the copy number of the CPMV RNA-2/ng total RNA (Figure 6B). Amplification efficiency above 90% was observed with correlation coefficient (R^2) > 0.99. In agreement with previous work analyzing CPMV after oral or intravenous (I.V.) administration,[60] we detected CPMV RNA-2 in all the organs independent of administration route (I.T. or O.G.) (Figure 6B,C). While broad biodistribution was apparent, the highest amount of CPMV was detected in the tumors after I.T. administration, mirroring the fluorescence analysis (Figures 5 and 6A).

While the majority of the I.T.-injected dose remains in the tumor, particles that leached were cleared by the liver, spleen, and kidneys with 2×10^7 and 3.8×10^7 copies of RNA-2/ng of total RNA for liver and spleen, respectively, and 1.8×10^7 copies of RNA-2/ng of total RNA for kidneys—in contrast, 5×10^8 copies of RNA-2/ng of total RNA were detected in the tumor. It was noted that independent of the route of administration, CPMV particles were found in the lungs. For the O.G. administration, CPMV nanoparticles were largely found in

the stomach, large intestine, and lungs. Overall, the results for Cy5-CPMV are in agreement with results from CPMV-treated animals, as expected (Figure 6B,C).

Our data are consistent with previous work on the biodistribution, toxicology, and pathology of CPMV assessed in mice.[73] In previous works, the CPMV fate was studied after I.V. administration, and the key reported findings are as follows: CPMV particles are cleared rapidly from plasma (~20–30 min). The majority of I.V.-administered CPMV is cleared by the liver and to a lesser extent by the spleen. At doses of up to 100 mg/kg body weight, no toxicity was noted. Hematology was essentially normal, although the mice were somewhat leukopenic. Histological examination of the spleen showed cellular infiltration, attributed to elevated B lymphocytes on the first day following I.V. administration of CPMV. Microscopic evaluation of various other tissues revealed a lack of apparent tissue degeneration or necrosis. The study concluded that CPMV appears to be a safe and nontoxic platform for in vivo biomedical applications at doses up to 100 mg/kg of body weight.[73] Our data also indicate broad biodistribution with clearance by the reticuloendothelial system and biliary (and lesser extend renal) excretion.

Next, we sought to address whether there was any evidence of shedding of infectious CPMV or noninfectious components thereof; that is, whether CPMV protein and/or RNA could be detected in urine and stool specimens by Western blot and RT-PCR, respectively (Figure 6D,E). PBS treatments were used as controls, and data are shown in Figure S1. Longitudinal Western blot tests did not indicate any evidence of CPMV coat proteins in urine or stool (Figure 6D and Figure S1C). RT-PCR did not detect any CPMV RNA-2 in urine after CPMV administration independent of the administration route. However, in stool, CPMV RNA-2 was detected after I.T. administration but not after O.G. More specifically, one out of every three samples tested positive for CPMV RNA-2 in stool (Figure 6D, lane 7). This suggests that, while there is no shedding of infectious particles after ingestion of plant viruses, RNA shedding in stool after I.T. administration is possible. Therefore, we tested whether there was any indication that stool (or urine) could contain CPMV that is infectious in plants.

Infectivity of Excreted CPMV toward Plants.

Using pooled urine and stool samples as well as CPMV and healthy plant controls, we mechanically inoculated primary leaves of black-eyed pea plants. Plants were monitored for the appearance of symptoms and photographed 10 days postinoculation. Visual inspection did not indicate symptoms on any leaves except the CPMV-infected positive control plants (Figures 7A and S2); the latter showed the typical mosaic and mottled yellow spots. To further validate this finding, we carried out Western blot and RT-PCR analysis on the plant sap extracted from individual leaves, and CPMV could not be detected, neither on the protein nor at the RNA level (Figure 7B,C), which suggests that the RNA detected in stool may not be infectious toward plants. This is congruent with data surrounding SARS-CoV-2, where viral RNA with a mitigated replicative capacity can be detected in stool samples.[74]

From a translational perspective, these data convey that shedding of infectious CPMV was not evident after I.T. or oral dosing. We sought to further investigate the fate of CPMV after administration via the oral route because previous work demonstrated that CPMV

is orally bioavailable[60] and is stable in gastric and intestinal fluids.[60,63] Our data are in agreement with previous reports showing that CPMV is detectable in all organs after O.G.[60] (see Figure 6C), albeit at low levels, and that anti-CPMV immunity was induced after O.G. (see Figure 4B). We probed the stability of CPMV under simulated gastric and intestinal fluids (SGF and SIF) with and without pepsin or pancreatin, GI tract enzymes. In contrast to bovine serum albumin (BSA) controls, CPMV remained somewhat stable under SGF and SIF conditions without GI enzymes (Figure S3), as per native gel electrophoresis and SDS-PAGE. However, CPMV particle instability and coat protein degradation were apparent within 1 h of exposure to pepsin, with no protein was detectable at 24 h of incubation (Figure S3A).[60,63] On the other hand, CPMV (but not BSA) was found to be more stable under SIF conditions with and without pancreatin (Figure S3B); while coat protein degradation was not apparent, the BSA control was digested. Interestingly, the CPMV RNA was not observed on the native agarose gels, despite the presence of coat proteins. This indicates protein stability but RNA instability under SIF conditions. Together, the data indicate limited stability of CPMV after the oral route and therefore limited risk of shedding of infectious particles after food consumption.

CONCLUSIONS

While plant virus nanotechnology is a small branch of the nanomedicine field,[21,75-77] several candidates have or are undergoing clinical testing (NCT03301051[78] and NCT03739112,[78] NCT02233816[79] and NCT0223602,[79] NCT01991561,[80] NCT0098494,[81] NCT04636697,[82] NCT02567955,[83] NCT00534638,[84] and NCT00090220[85]), which shows that the technology has matured. Plant viruses are biologics, but they are also nanoparticles as their capsids are nanoscale materials self-assembled from a coat protein unit. Here, we focused on translational studies for development of CPMV as an in situ vaccine for cancer therapy. In prior work, we discovered that intratumoral CPMV nanoparticles prime potent, durable, systemic antitumor immunity with demonstrated efficacy in mouse models and canine patients.[26,30-32] The work presented here was motivated as a prelude toward investigational new drug (IND)-enabling toxicology studies. We analyzed prevalence of anti-CPMV antibodies in humans and performed biodistribution and clearance studies to gain insight into the pharmacology and fate of CPMV (i.e., determine the degree of leaching and whether shedding occurs).

Our data indicate the prevalence of anti-CPMV antibodies in humans, which would indicate human exposure—likely through food consumption. There was no correlation between plant virus in the U.S. or global distribution and antibody prevalence in humans, and data indicate that other factors, such as virus particle stability, may come into play. Limitations of the present data are the small cohort of patients (50 patients) and lack of information about residence and travel abroad or dietary information. CPMV has limited global distribution and is principally found in Nigeria and Uganda—in the U.S., it has been reported in Missouri, Texas, and Michigan.[53] Therefore, it would be important to understand whether patients who consume cowpeas and who have traveled or reside in areas where CPMV is found have a higher likelihood for CPMV antibodies versus patients that do not consume legumes susceptible to CPMV infection. Further, a growing body of data suggests that plant viruses are an integral component of the microbiome.[45-48,86,87] With

plant viruses advancing toward human clinical applications, more research is needed to gain a fundamental understanding of the plant virus–human interactions. From a translational perspective, the prevalence of anti-CPMV antibodies is not expected to be a hurdle: previous research demonstrated that anti-CPMV antibodies are not neutralizing the efficacy of CPMV-ISV.[50] Nevertheless, clinical protocols should consider that some humans (>50% of patients with the pool analyzed) present with anti-CPMV antibodies; even if patients test negative for anti-CPMV antibodies, repeat ISV treatment will lead to humoral[50] and cellular immunity[28] against CPMV.

We analyzed the biodistribution and clearance of CPMV after I.T. and O.G. dosing. Data demonstrate prolonged retention in the tumor after I.T. treatment, with minimal leaching observed. While biodistribution was broad with all major organs testing positive for CPMV after I.T. or O.G. administration, concentrations of CPMV in all tissues but the tumor were low. Clearance via the reticuloendothelial system followed by biliary (and lesser extend renal) excretion was indicated. Genomic CPMV RNA-2 was detectable only in some stool samples after I.T. treatment in tumor-bearing mice, but there was no evidence of protein shedding, and RNA was not infectious toward black-eyed pea plants when these samples were mechanically inoculated on their leaves.

It is important to note that there are limitations to the data presented, and this body of work should be considered a prelude toward IND-enabling toxicology: first, even though we found that there is minimal leaching of intratumorally administered CPMV from the B16F10 dermal tumors, one may consider assessing the degree of leaching in several tumor types with varying degrees of vascularization; the degree of leaching from the tumor may also be influenced by the injection volume and technique. Second, while previous data indicate the safety of CPMV in mice after intravenous injection at doses up to 100 mg/kg of body weight,[73] detailed organs and immunological toxicity after intratumoral administration should be carefully considered, and this will be part of IND-enabling toxicology studies. Lastly, our data indicate that presence CPMV RNA in some stool samples from mice receiving intratumoral CPMV; however, the pooled stool samples were not infectious toward cowpea plants. Future studies may consider testing additional plant species and analyzing a larger cohort of mice or large animals. For example, in ongoing work, we are testing the CPMV-ISV in canine patients with spontaneous tumors, and blood and urine/stool samples will be analyzed to gain further insight into pharmacology of CPMV.

Taken together, these results reported here provide insights of human exposure to CPMV as evidenced by the presence of anti-CPMV antibodies. We provide insights into the pharmacology of CPMV and observed that CPMV has good tumor retention properties (attesting to its nanoparticle features) with minimal systemic exposure; shedding of infectious CPMV was not detected. We propose live CPMV as a drug candidate for human clinical trials, and these data indicate the agronomical safety of CPMV cancer immunotherapy.

METHODS

Cowpea Mosaic Virus Propagation and Preparation of Cy5-CPMV.

CPMV was propagated in black-eyed pea No. 5 plants (*Vigna unguiculata*) by mechanical inoculation and purified as reported in previous work.[88] *N*-Hydroxysuccinimide chemistry was used to conjugate fiuorescent dye cyanine-5 succinimide ester (NHS-sulfo-Cy5; Lumiprobe) to CPMV's surface lysine residues to obtain Cy5-CPMV. Briefly, 900 molar excess of NHS-sulfo-Cy5 was added to the CPMV in 10 mM potassium phosphate (KP) buffer (2 mg·mL^{-1}) and mixed at room temperature for 2 h, protected from light.[50] The solution was ultracentrifuged at 4 °C at 52000*g* for 1 h over a 30% (w/v) sucrose cushion. The resulting pellet was resuspended in 10 mM KP and stored at 4 °C until further characterization.

Tobacco Mosaic Virus, Potato Virus X, Chlorotic Cowpea Mosaic Virus Propagation, and Qβ VLP Production and Characterization.

TMV,[89] CCMV,[90] and PVX[91] were propagated in plants and purified using our established protocols. Bacteriophage Qβ VLPs were expressed in BL21 *Escherichia coli* and purified as previously reported.[92] Characterization of the plant viruses and VLPs was reported elsewhere.[89,90,92-94]

CPMV and Cy5-CPMV Characterization.

UV–Vis.—CPMV concentration and the degree of Cy5 labeling were determined using a UV–vis Nanodrop 2000 (Thermo Fisher Scientific). The concentration of CPMV and Cy5-CPMV was calculated using Beer–Lambert law with the extinction coefficient of CPMV at 260 nm (ε_{CPMV} = 8.1 L mol^{-1} cm^{-1}) and Cy5 at 647 nm (ε_{Cy5} = 270,000 L mol^{-1} cm^{-1}).

Agarose Gel Electrophoresis.—A total of 6× gel loading purple dye (Biolabs) was added to CPMV and Cy5-CPMV particles (10 μg) and then loaded onto a 1.2% (w/v) agarose gel stained with GelRed (Gold Biotechnologies) in TAE buffer (gels were run for 30 min at 120 V and 400 mA). Gels were imaged under UV light to visualize the RNA, MultiFluor Red channel (607 nm excitation) to image the Cy5 dye, and then stained with Coomassie Brilliant Blue G-250 (0.25% w/v) and imaged under white light to detect the protein.

SDS-Gel Electrophoresis.—CPMV and Cy5-CPMV (10 μg) were loaded with 4× lithium dodecyl sulfate sample buffer (Life Technologies) and 10× NuPAGE sample reducing agent (Invitrogen). The particles were denatured (95 °C, 5 min) and analyzed on NuPAGE 4–12% bis-Tris protein gel (Invitrogen) in 1× morpholinepropanesulfonic acid (MOPS) buffer (ThermoFisher Scientific) (200 V, 120 mA, and 25 W for 40 min). The gel was imaged using the MultiFluor Red channel and then stained with GelCode Blue Safe protein stain and visualized under white light to image both the Cy5 label and CPMV's coat proteins.

Dynamic Light Scattering.—The hydrodynamic diameters of CPMV and Cy5-CPMV were assessed using a Zetasizer Nano ZSP/Zen5600 (Malvern Panalytical) at 25 °C with

three measurements per sample; the particle diameter was calculated as the weighted mean of the intensity distribution.

Transmission Electron Microscopy.—Formvar carbon film-coated TEM supports with 400-mesh hexagonal copper grids (VWR International) were rendered more hydrophilic using the PELCO easiGlow operating system. CPMV and Cy5-CPMV (0.1 $mg \cdot mL^{-1}$ in DI H_2O) were loaded onto the grids and then stained with 2% (w/v) uranyl acetate (Agar Scientific). The samples were imaged using a FEI TecnaiSpirit G2 BioTWIN TEM at 80 kV.

Size Exclusion Chromatography.—CPMV and Cy5-CPMV (0.5 mg/mL) were analyzed on an ÄKTA pure fast protein liquid chromatography system (GE Healthcare LifeSciences) using a Superose 6 increase column size-exclusion column at a 0.5 mL min^{-1} flow rate. The elution profile was isocratic, and the UV detectors were fixed at 260 (nucleic acid), 280 (protein), and 647 nm (Cy5).

Detection of Anti-VNP/VLP Antibodies in Human Plasma.

ELISA was used to detect levels of VNP/VLP-specific IgG in human plasma generously provided by UC San Diego Research Biobank (Altman Clinical and Translational Research Institute). The 96-well microplates (Nunc MaxiSorp flat-bottom, Thermo Fisher Scientific) were coated with 1 μg of VNPs/VLP in their appropriate buffer (Table 1) and incubated overnight at 4 °C. Plates were washed three times with washing buffer (0.05% (v/v) Tween-20 in PBS, 300 μL per well) after coating and between all subsequent steps. The plate was then blocked with 200 μL of blocking solution (3% (w/v) BSA, in PBS) and placed in a microplate shaker incubator (37 °C, 1 h). Plasma from human patients was added to the wells in 1:200 serial dilutions, and 1:1000 dilution of respective rabbit anti-VNP/VLP antibody (Pacific Immunology) was used as a positive control (100 μL/well, 1% (w/v) BSA in PBS). As a negative control, no plasma sample was added to the wells, followed by the addition of 100 μL/well of 1% (w/v) BSA in PBS. Plates were then incubated (37 °C, 1h) in a microplate shaker incubator. Next, after the plates were washed three times with washing buffer, they were incubated with 1:5000 dilution (100 μL/well, 1% (w/v) BSA in PBS) of horseradish peroxidase (HRP)-labeled rabbit anti-human IgG Fc (Novus Biologicals) for human plasma wells and HRP-labeled goat anti-rabbit IgG (H+L) (Fisher Scientific) for VNP/VLP positive control wells, respectively. The wells were developed with 100 μL of 1-Step Ultra TMB-ELISA substrate solution (Thermo Fisher Scientific) for 2 min at room temperature and quenched with 50 μL of 2 N sulfuric acid (Spectrum Chemical). Absorbance was read at 450 nm using the Infinite 200 Pro microplate reader and the software i-control (Tecan, Männedorf, Switzerland).

Tumor Model and Biodistribution Study.

All animals used in this study were 7–8 week old female C57BL/6 mice obtained from The Jackson Laboratory (Strain #000664). All animal experiments were carried out in accordance with the University of California San Diego's Institutional Animal Care and Use Committee (IACUC).

Murine B16F10 melanoma cells (ATCC) were maintained at 37 °C (5% CO_2) in Dulbecco's modified Eagle's medium (Corning, 10-017-CV) supplemented with 10% (v/v) fetal bovine serum (Cytiva, SH30071.02) and 100 units/mL penicillin and 100 μg/mL streptomycin (Cytiva, SV30010). B16F10 cells (200,000 cells in 30 μL of sterile PBS, Corning, 21-040-CV) were administered dermally into the right flank. Mice were monitored daily for signs of tumor progression. When tumors were palpable and reached 30 mm^3, CPMV or Cy5-CPMV (n = 4, 100 μg in 20 μL of PBS) were administered I.T., three times, every 5 days. PBS (20 μL) and free sulfo-cyanine-5 normalized to Cy5-CPMV were used as controls. For O.G., mice were fasted for 4 h prior to O.G.; animals received three treatments every 5 days using CPMV or Cy5-CPMV (n = 4, 100 μg in 300 μL of sterile PBS).

For live animal imaging studies, mice were imaged using the IVIS Spectrum Imaging System (PerkinElmer Ltd.) 1 h after every I.T. injection and then daily until the next treatment. Cy5 fluorescence was determined using Living Image software (PerkinElmer Ltd.). Regions of interest were quantified as average radiance (photons/s).

For ex vivo biodistribution studies, mice were euthanized 24 h after the third I.T. injection or O.G. Heart, brain, lung, stomach, spleen, liver, kidneys, large and small intestines, and tumors were collected and kept in RNA*later* stabilization solution (Thermo Fisher Scientific) at −20 °C until further analysis. Collection of mice urine and stool was performed using metabolic cages. Samples were collected for 4 h before treatment and four post-24 h after treatment, which was either I.T. using tumor-bearing mice or O.G. using healthy mice. Samples were stored at −20 °C until further analysis.

For fluorescence measurements, frozen organs from Cy5-CPMV-treated animals and controls were thawed, cut, weighed, and mixed with PBS (100 mg organ/mL PBS). They were then homogenized using a gentleMACS dissociator (Miltenyi Biotec) and centrifuged at 3000*g* for 5 min to remove tissue debris. The Cy5-specific fluorescence emissions (λ_{Ex} = 633 nm and λ_{Em} = 665 nm) in the clarified tissue supernatants were determined using the Infinite 200 Pro microplate reader and the software i-control (Tecan, Männedorf, Switzerland). Organs from CPMV-treated animals were analyzed by RT-qPCR as described below.

RNA Extraction from Organs, Stool, Urine, and Plant Sap.

RNA extraction from organs was performed using an RNAqueous kit according to the manufacturer's protocol. Briefly, organs were cut, weighed, and thoroughly homogenized using 10–12 $\mu L \cdot mg^{-1}$ of tissue lysis/binding solution using a gentleMACS dissociator.

Urine collected from mice was centrifuged at 1500*g* for 10 min to pellet down any cellular material. Stool was diluted in sterile PBS (Corning, 21-040-CV) and centrifuged at 4000*g* for 20 min to obtain a supernatant. Processed urine and stool were kept at −80 °C before RNA extraction.

Cowpea (*V. unguiculata*) leaves (see below) were also analyzed: leaves were pulverized under liquid nitrogen using a mortar and pestle. The resulting leaf powder was suspended into 1 mL of KP (0.1 M, pH 7) per gram of leaf material. The mixture was filtered through

two layers of miracloth and centrifuged at 13,000*g* for 10 min to recover plant sap that was kept at −20 °C before RNA extraction.

RNA extraction from urine, stool, and plant sap was performed using a QIAamp Viral RNA mini kit (cat. no. 52904) according to manufacturer's protocol. RNA purity and concentration were quantified using a Thermo Scientific Nanodrop 2000 spectrophotometer at a ratio of 260/280 and 260/230 and kept at −80 °C until further analysis. Pure RNA should yield around 2 or higher for both ratios.

Reverse Transcription and (Quantitative) Polymerase Chain Reaction (RT-qPCR).

RT-qPCR on RNA from Organs.—RT-qPCR on RNA-extracted organs was performed using TaqMan Fast Virus 1-Step Master Mix (cat. no. 444432) according to manufacturer's protocol. The CPMV TaqMan gene expression assay (20×) was designed using the IDT PrimerQuest tool. The expression assay consisted of a probe (5′-/56-FAM/TATAGCTCC/ZEN/AAGCAAGCGGGAACC/3IABkFQ/-3′), a reverse primer (5′-CATGGGCTATACACATCTGAGG-3′), and a forward primer (5′-GGTATAGGTTCTAATCCGGGTATTG-3). The ratio of primers to probe is 2:1. The RT-qPCR reactions were performed on BioRad CFX96 touch real-time PCR detection system. All samples were run in triplicate. Quantification cycle (C_q) values were tabulated by CFX Maestro software.

RT-qPCR Standard Curve Using CPMV RNA.—Standard curve was constructed using CPMV RNAs extracted from wild-type CPMV. Serial dilutions of CPMV RNAs (100, 10, 1, 0.1, and 0.01 ng) and NTC (no template control) were used as templates to perform RT-qPCR as described above. All samples were run in triplicate. Quantification cycle (C_q) values, PCR efficiency (E), and correlation coefficient (R^2) were tabulated by CFX Maestro software.

RT-PCR on RNAs from Urine, Stool, and Plant Sap.—RT-PCR on RNA extracted urine and stool was performed using Invitrogen SuperScript IV one-step RT-PCR (cat. no. 12594100) according to manufacturer's protocol. The RT-PCR reactions were performed on a BioRad T100 PCR detection system. All samples were run in triplicate. PCR products were analyzed on 1.2% (w/v) TAE agarose gel.

Western Blot on Stool, Urine, and Plant Sap Samples.

Total protein in urine and stool samples was quantified using a Pierce BCA protein assay (cat. no. 23277) in triplicate according to manufacturer's protocol. Forty micrograms of total protein from urine and stool samples and 10 μL of plant sap extract supernatant were separated on 4–12% SDS-PAGE precast gels in 1× MOPS buffer (Thermo Fisher Scientific) for 40 min at 200 V and 120 mA. SeeBlue Plus2 (Thermo Fisher Scientific) was used as a marker. Proteins were then electrotransferred onto a nitrocellulose membrane (Amersham Protran Premium 0.45 μm nitrocellulose, GE Healthcare). The membranes were blocked with 5% (w/v) BSA in PBS (room temperature, 1 h) and then washed with PBS. Primary antibody incubation proceeded with 1:1000 dilution of rabbit anti-CPMV polyclonal antibody (PAC 12273/12274) in 5% (w/v) BSA in PBS with 0.05% (v/v)

Tween-20 (PBS-T buffer at room temperature, 1 h) followed by washing three times with PBS-T. Secondary antibody incubation proceeded with HRP-labeled goat anti-rabbit IgG (H+L) (Fisher Scientific) in 2% (w/v) BSA in 1× PBS-T (room temperature, 1 h) followed by washing three times with PBS-T and one time with PBS. Membranes were developed using Thermo Scientific Pierce ECL Western Blotting substrate for 1 min and imaged using chemiluminescence on ProteinSimple FluorChem R.

Detection of Anti-CPMV Antibodies in Mice Plasma.

Blood samples were collected through retro-orbital bleeding before any I.T./O.G. procedure (i.e., prebleed) and then right before the second, third, and post-24 h after the last I.T./O.G. procedure (referred to as first, second, and third I.T./O.G. bleed). Serial plasma dilutions (1:200 to 1:204,800) were tested for anti-CPMV antibodies using ELISA as described above, except that we used 1:5000 HRP-labeled goat anti-mouse IgG H+L (Invitrogen) as the secondary antibody.

Infectivity of CPMV from Stool and Urine in Plants.

Seven days after seeding, primary leaves of *V. unguiculata* (California black-eye bush beans No. 5) were mechanically inoculated with carborundum (Thermo Fisher Scientific) and 20 μL per leaf of pooled stool or urine samples from O.G. or I.T.-treated animals. Pretreatment samples served as negative controls, and CPMV served as a positive control; for the latter, leaves were dusted with carborundum and inoculated using 20 μL per leaf of 0.1 $mg \cdot mL^{-1}$ CPMV in 10 mM KP. Leaves were photographed and harvested 10 days postinoculation and stored at −80 °C until further experiments.

Supplementary Material

Refer to Web version on PubMed Central for supplementary material.

ACKNOWLEDGMENTS

This work was supported in part through NIH Grants R01 CA224605, R01 CA253615, U01 CA218292, and R01 CA274640 (to N.F.S.). N.F.S. acknowledges support through the Shaughnessy Family Fund for Nano-ImmunoEngineering (nanoIE) at UCSD as well as a UC San Diego Galvanizing Engineering in Medicine (GEM) Award. A.O.O. acknowledges support from San Diego Fellowship and the Alfred P. Sloan Foundation's Minority PhD (MPhD) Program (G-2020-14067).

REFERENCES

(1). Rizzo LY; Theek B; Storm G; Kiessling F; Lammers T Recent Progress in Nanomedicine: Therapeutic, Diagnostic and Theranostic Applications. Curr. Opin. Biotechnol 2013, 24, 1159–1166. [PubMed: 23578464]

(2). Shreffler JW; Pullan JE; Dailey KM; Mallik S; Brooks AE, Overcoming Hurdles in Nanoparticle Clinical Translation: The Influence of Experimental Design and Surface Modification. Int. J. Mol. Sci 2019, 20, 6056. [PubMed: 31801303]

(3). Duncan R; Gaspar R Nanomedicine(s) under the Microscope. Mol. Pharmaceutics 2011, 8, 2101–2141.

(4). Rybicki EP Plant Molecular Farming of Virus-like Nanoparticles as Vaccines and Reagents. Wiley Interdiscip. Rev. Nanomedicine Nanobiotechnology 2020, 12, e1587. [PubMed: 31486296]

(5). Buyel JF Plant Molecular Farming – Integration and Exploitation of Side Streams to Achieve Sustainable Biomanufacturing. Front. Plant Sci 2019, 9, 1–17.

(6). Daniell H; Streatfield SJ; Wycoff K Medical Molecular Farming: Production of Antibodies, Biopharmaceuticals and Edible Vaccines in Plants. Trends Plant Sci. 2001, 6, 219–226. [PubMed: 11335175]

(7). Fischer R; Drossard J; Commandeur U; Schillberg S; Emans N Towards Molecular Farming in the Future: Moving from Diagnostic Protein and Antibody Production in Microbes to Plants. Biotechnol. Appl. Biochem 1999, 30, 101–108. [PubMed: 10512787]

(8). Narayanan KB; Han SS Icosahedral Plant Viral Nanoparticles - Bioinspired Synthesis of Nanomaterials/Nanostructures. Adv. Colloid Interface Sci 2017, 248, 1–19. [PubMed: 28916111]

(9). Lico C; Benvenuto E; Baschieri S The Two-Faced Potato Virus X: From Plant Pathogen to Smart Nanoparticle. Front. Plant Sci 2015, 6, 1–8. [PubMed: 25653664]

(10). Yuste-Calvo C; González-Gamboa I; Pacios LF; Sánchez F, Ponz F. Structure-Based Multifunctionalization of Flexuous Elongated Viral Nanoparticles. ACS Omega 2019, 4, 5019–5028.

(11). Lee KL; Hubbard LC; Hern S; Yildiz I; Gratzl M; Steinmetz NF Shape Matters: The Diffusion Rates of TMV Rods and CPMV Icosahedrons in a Spheroid Model of Extracellular Matrix Are Distinct. Biomater. Sci 2013, 1, 581.

(12). Venkataraman S; Hefferon K Application of Plant Viruses in Biotechnology, Medicine, and Human Health. Viruses 2021, 13, 1697. [PubMed: 34578279]

(13). Rohovie MJ; Nagasawa M; Swartz JR Virus-like Particles: Next-Generation Nanoparticles for Targeted Therapeutic Delivery. Bioeng. Transl. Med 2017, 2, 43–57. [PubMed: 29313023]

(14). Nooraei S; Bahrulolum H; Hoseini ZS; Katalani C; Hajizade A; Easton AJ; Ahmadian G Virus-like Particles: Preparation, Immunogenicity and Their Roles as Nanovaccines and Drug Nanocarriers. J. Nanobiotechnology 2021, 19, 59. [PubMed: 33632278]

(15). Li L; Xu C; Zhang W; Secundo F; Li C; Zhang Z-P; Zhang X-E; Li F Cargo-Compatible Encapsulation in Virus-Based Nanoparticles. Nano Lett. 2019, 19, 2700–2706. [PubMed: 30895793]

(16). Chung YH; Cai H; Steinmetz NF Viral Nanoparticles for Drug Delivery, Imaging, Immunotherapy, and Theranostic Applications. Adv. Drug Delivery Rev 2020, 156, 214–235.

(17). Mohsen MO; Speiser DE; Knuth A; Bachmann MF Virus-like Particles for Vaccination against Cancer. WIREs Nanomedicine and Nanobiotechnology 2020, 12, e1579. [PubMed: 31456339]

(18). Kaufman HL; Kohlhapp FJ; Zloza A Oncolytic Viruses: A New Class of Immunotherapy Drugs. Nat. Rev. Drug Discovery 2015, 14, 642–662. [PubMed: 26323545]

(19). de Almeida NAA; Ribeiro C. R. d. A.; Raposo JV; de Paula VS Immunotherapy and Gene Therapy for Oncoviruses Infections: A Review. Viruses 2021, 13, 822. [PubMed: 34063186]

(20). Tian Y; Xie D; Yang L Engineering Strategies to Enhance Oncolytic Viruses in Cancer Immunotherapy. Signal Transduct. Target. Ther 2022, 7, 117. [PubMed: 35387984]

(21). Royal JM; Simpson CA; McCormick AA; Phillips A; Hume S; Morton J; Shepherd J; Oh Y; Swope K; Debeauchamp JL; et al. Development of a SARS-CoV-2 Vaccine Candidate Using Plant-Based Manufacturing and a Tobacco Mosaic Virus-like Nano-Particle. Vaccines 2021, 9, 1347. [PubMed: 34835278]

(22). Mohsen MO; Zha L; Cabral-Miranda G; Bachmann MF Major Findings and Recent Advances in Virus–like Particle (VLP)-Based Vaccines. Semin. Immunol 2017, 34, 123–132. [PubMed: 28887001]

(23). Ribas A; Medina T; Kirkwood JM; Zakharia Y; Gonzalez R; Davar D; Chmielowski B; Campbell KM; Bao R; Kelley H; et al. Overcoming PD-1 Blockade Resistance with CpG-A Toll-like Receptor 9 Agonist Vidutolimod in Patients with Metastatic Melanoma. Cancer Discov 2021, 11, 2998–3007. [PubMed: 34326162]

(24). Lemke-miltner CD; Blackwell SE; Yin C; Krug AE; Morris AJ; Krieg AM; Weiner GJ Antibody Opsonization of a TLR9-Agonist-Containing Virus-like Particle Enhances in Situ Immunization. J. Immunol 2020, 204, 1386–1394. [PubMed: 31953355]

(25). Maharjan PM; Choe S Plant-Based COVID-19 Vaccines: Current Status, Design, and Development Strategies of Candidate Vaccines. Vaccines 2021, 9, 992. [PubMed: 34579229]

(26). Beiss V; Mao C; Fiering SN; Steinmetz NF Cowpea Mosaic Virus Outperforms Other Members of the Secoviridae as In Situ Vaccine for Cancer Immunotherapy. Mol. Pharmaceutics 2022, 19, 1573–1585.

(27). Shukla S; Wang C; Beiss V; Cai H; Washington T; Murray AA; Gong X; Zhao Z; Masarapu H; Zlotnick A; et al. The Unique Potency of Cowpea Mosaic Virus (CPMV): In Situ Cancer Vaccine. Biomater. Sci 2020, 8, 5489–5503. [PubMed: 32914796]

(28). Wang C; Fiering SN; Steinmetz NF Cowpea Mosaic Virus Promotes Anti-Tumor Activity and Immune Memory in a Mouse Ovarian Tumor Model. Adv. Ther 2019, 2, 1900003.

(29). Kerstetter-Fogle A; Shukla S; Wang C; Beiss V; Harris PLR; Sloan AE; Steinmetz NF Plant Virus-like Particle in Situ Vaccine for Intracranial Glioma Immunotherapy. Cancers (Basel) 2019, 11, 515. [PubMed: 30974896]

(30). Hoopes PJ; Wagner RJ; Duval K; Kang K; Gladstone DJ; Moodie KL; Crary-Burney M; Ariaspulido H; Veliz FA; Steinmetz NF; et al. Treatment of Canine Oral Melanoma with Nanotechnology-Based Immunotherapy and Radiation. Mol. Pharmaceutics 2018, 15, 3717–3722.

(31). Alonso-Miguel D; Valdivia G; Guerrera D; Perez-Alenza MD; Pantelyushin S; Alonso-Diez A; Beiss V; Fiering S; Steinmetz NF; Suarez-Redondo M; et al. Neoadjuvant in Situ Vaccination with Cowpea Mosaic Virus as a Novel Therapy against Canine Inflammatory Mammary Cancer. J. Immunother. Cancer 2022, 10, e004044. [PubMed: 35277459]

(32). Lizotte PH; Wen AM; Sheen MR; Fields J; Rojanasopondist P; Steinmetz NF; Fiering S In Situ Vaccination with Cowpea Mosaic Virus Nanoparticles Suppresses Metastatic Cancer. Nat. Nanotechnol 2016, 11, 295–303. [PubMed: 26689376]

(33). Mao C; Beiss V; Fields J; Steinmetz NF; Fiering S Cowpea Mosaic Virus Stimulates Antitumor Immunity through Recognition by Multiple MYD88-Dependent Toll-like Receptors. Biomaterials 2021, 275, 120914. [PubMed: 34126409]

(34). Wang C; Beiss V; Steinmetz NF Cowpea Mosaic Virus Nanoparticles and Empty Virus-Like Particles Show Distinct but Overlapping Immunostimulatory Properties. J. Virol 2019, 93, 1–14.

(35). Huynh NT; Hesketh EL; Saxena P; Meshcheriakova Y; Ku Y-C; Hoang LT; Johnson JE; Ranson NA; Lomonossoff EP; Reddy VS Crystal Structure and Proteomics Analysis of Empty Virus-like Particles of Cowpea Mosaic Virus. Structure 2016, 24, 567–575. [PubMed: 27021160]

(36). Saunders K; Sainsbury F; Lomonossoff GP Efficient Generation of Cowpea Mosaic Virus Empty Virus-like Particles by the Proteolytic Processing of Precursors in Insect Cells and Plants. Virology 2009, 393, 329–337. [PubMed: 19733890]

(37). Koellhoffer EC; Mao C; Beiss V; Wang L; Fiering SN; Boone CE; Steinmetz NF Inactivated Cowpea Mosaic Virus in Combination with OX40 Agonist Primes Potent Antitumor Immunity in a Bilateral Melanoma Mouse Model. Mol. Pharmaceutics 2022, 19, 592–601.

(38). Chariou PL; Beiss V; Ma Y; Steinmetz NF In Situ Vaccine Application of Inactivated CPMV Nanoparticles for Cancer Immunotherapy. Mater. Adv 2021, 2, 1644–1656. [PubMed: 34368764]

(39). Lomonossoff GP Cowpea Mosaic Virus. Encycl. Virol 2008, 2005, 569–574.

(40). Chatzivassiliou EK An Annotated List of Legume-Infecting Viruses in the Light of Metagenomics. Plants 2021, 10, 1413. [PubMed: 34371616]

(41). Gergerich RC; Dolja VV Introduction to Plant Viruses, the Invisible Foe. Plant Heal. Instr 2006, DOI: 10.1094/PHI-I-2006-0414-01.

(42). Jones RAC. Global Plant Virus Disease Pandemics and Epidemics. Plants 2021, 10, 233. [PubMed: 33504044]

(43). Rubio L; Galipienso L; Ferriol I Detection of Plant Viruses and Disease Management: Relevance of Genetic Diversity and Evolution. Front. Plant Sci 2020, 11, 1–23. [PubMed: 32117356]

(44). Amari K; Huang C; Heinlein M Potential Impact of Global Warming on Virus Propagation in Infected Plants and Agricultural Productivity. Front. Plant Sci 2021, 12, 1–7.

(45). Colson P; Richet H; Desnues C; Balique F; Moal V; Grob JJ; Berbis P; Lecoq H; Harlé JR; Berland Y; et al. Pepper Mild Mottle Virus, a Plant Virus Associated with Specific Immune Responses, Fever, Abdominal Pains, and Pruritus in Humans. PLoS One 2010, 5, e10041. [PubMed: 20386604]

(46). Aguado-García Y; Taboada B; Morán P; Rivera-Gutiérrez X; Serrano-Vázquez A; Iša P; Rojas-Velázquez L; Pérez-Juárez H; López S; Torres J; et al. Tobamoviruses Can Be Frequently Present in the Oropharynx and Gut of Infants during Their First Year of Life. Sci. Rep 2020, 10, 13595. [PubMed: 32788688]

(47). Zhang T; Breitbart M; Lee WH; Run JQ; Wei CL; Soh SWL; Hibberd ML; Liu ET; Rohwer F; Ruan Y RNA Viral Community in Human Feces: Prevalence of Plant Pathogenic Viruses. PLoS Biol. 2005, 4, e3.

(48). Balique F; Lecoq H; Raoult D; Colson P Can. Plant Viruses Cross the Kingdom Border and Be Pathogenic to Humans? Viruses 2015, 7, 2074–2098. [PubMed: 25903834]

(49). Chatterji A; Ochoa WF; Paine M; Ratna BR; Johnson JE; Lin T New Addresses on an Addressable Virus Nanoblock: Uniquely Reactive Lys Residues on Cowpea Mosaic Virus. Chem. Biol 2004, 11, 855–863. [PubMed: 15217618]

(50). Shukla S; Wang C; Beiss V; Steinmetz NF Antibody Response against Cowpea Mosaic Viral Nanoparticles Improves in Situ Vaccine Efficacy in Ovarian Cancer. ACS Appl. Mater. Interfaces 2020, 14, 2994–3003.

(51). Liu R; Vaishnav RA; Roberts AM; Friedland RP Humans Have Antibodies against a Plant Virus: Evidence from Tobacco Mosaic Virus. PLoS One 2013, 8, e60621. [PubMed: 23573274]

(52). Verchot J Potato Virus X: A Global Potato-Infecting Virus and Type Member of the Potexvirus Genus. Mol. Plant Pathol 2022, 23, 315–320. [PubMed: 34791766]

(53). Sastry KS; Bikash M; Hammond J; Scott SW; Briddon RW Encyclopedia of Plant Viruses and Viroids; Springer: New Delhi, 2019.

(54). Whitney WK; Gilmer RM Insect Vectors of Cowpea Mosaic Virus in Nigeria. Ann. Appl. Biol 1974, 77, 17–21. [PubMed: 4470367]

(55). Berzitis EA; Minigan JN; Hallett RH; Newman JA Climate and Host Plant Availability Impact the Future Distribution of the Bean Leaf Beetle (Cerotoma Trifurcata). Glob. Chang. Biol 2014, 20, 2778–2792. [PubMed: 24616016]

(56). CABI. Invasive Species Compend. UK CAB Int.: Wallingford, CT, 2022; http://www.cabi.org/isc.

(57). Widely Prevalent Virus of the United States, 2022; https://www.prevalentviruses.org/index.html.

(58). Verchot J Potato Virus X: A Global Potato-Infecting Virus and Type Member of the Potexvirus Genus. Mol. Plant Pa 2022, 23, 315–320.

(59). Le DHT; Lee KL; Shukla S; Commandeur U; Steinmetz NF Potato Virus X, a Filamentous Plant Viral Nanoparticle for Doxorubicin Delivery in Cancer Therapy. Nanoscale 2017, 9, 2348–2357. [PubMed: 28144662]

(60). Rae CS; Wei Khor I; Wang Q; Destito G; Gonzalez MJ; Singh P; Thomas DM; Estrada MN; Powell E; Finn MG; Manchester M; et al. Systemic Trafficking of Plant Virus Nanoparticles in Mice via the Oral Route. Virology 2005, 343, 224–235. [PubMed: 16185741]

(61). Kyriakopoulou PE; Kaponi MS; Boubourakas II; Hadidi A Plant and Green Microalgae Viruses in Human Diseases. Appl. Plant Virol. Adv. Detect. Antivir. Strateg 2020, 565–569.

(62). Van Regenmortel MH Tobacco Mosaic Virus (Virgaviridae). Encycl. Virol 2021, 3, 727–733.

(63). Berardi A; Evans DJ; Baldelli Bombelli F; Lomonossoff GP Stability of Plant Virus-Based Nanocarriers in Gastrointestinal Fluid. Nanoscale 2018, 10, 1667–1679. [PubMed: 29231944]

(64). Lavelle L; Michel J; Gingery M The Disassembly, Reassembly and Stability of CCMV Protein Capsids. J. Virol. Methods 2007, 146, 311–316. [PubMed: 17804089]

(65). Atabekov J; Dobrov E; Karpova O; Rodionova N Potato Virus X: Structure, Disassembly and Reconstitution. Mol. Plant Pathol 2007, 8, 667–675. [PubMed: 20507529]

(66). Loison P; Majou D; Gelhaye E; Boudaud N; Gantzer C Impact of Reducing and Oxidizing Agents on the Infectivity of Qβ Phage and the Overall Structure of Its Capsid. FEMS Microbiol. Ecol 2016, 92, fiw153. [PubMed: 27402711]

(67). Boone CE; Wang C; Lopez-Ramirez MA; Beiss V; Shukla S; Chariou PL; Kupor D; Rueda R; Wang J; Steinmetz NF Active Microneedle Administration of Plant Virus Nanoparticles for Cancer In Situ Vaccination Improves Immunotherapeutic Efficacy. ACS Appl. Nano Mater 2020, 3, 8037–8051. [PubMed: 33969278]

(68). Czapar AE; Tiu BDB; Veliz FA; Pokorski JK; Steinmetz NF Slow-Release Formulation of Cowpea Mosaic Virus for In Situ Vaccine Delivery to Treat Ovarian Cancer. Adv. Sci 2018, 5, 1700991.

(69). Gadd AJR; Greco F; Cobb AJA; Edwards AD Targeted Activation of Toll-Like Receptors: Conjugation of a Toll-Like Receptor 7 Agonist to a Monoclonal Antibody Maintains Antigen Binding and Specificity. Bioconjugate Chem. 2015, 26, 1743–1752.

(70). Steinmetz NF; Cho C-F; Ablack A; Lewis JD; Manchester M Cowpea Mosaic Virus Nanoparticles Target Surface Vimentin on Cancer Cells. Nanomedicine 2011, 6, 351–364. [PubMed: 21385137]

(71). Carette JE; Guhl K; Wellink J; Van Kammen A Coalescence of the Sites of Cowpea Mosaic Virus RNA Replication into a Cytopathic Structure. J. Virol 2002, 76, 6235–6243. [PubMed: 12021357]

(72). Kruse I; Peyret H; Saxena P; Lomonossoff GP Encapsidation of Viral RNA in Picornavirales: Studies on Cowpea Mosaic Virus Demonstrate Dependence on Viral Replication. J. Virol 2019, 93, 1–19.

(73). Singh P; Prasuhn D; Yeh RM; Destito G; Rae CS; Osborn K; Finn MG; Manchester M Bio-Distribution, Toxicity and Pathology of Cowpea Mosaic Virus Nanoparticles in Vivo. J. Controlled Release 2007, 120, 41–50.

(74). Cerrada-Romero C; Berastegui-Cabrera J; Camacho-Martinez P; Goikoetxea-Aguirre J; Perez-Palacios P; Santibanez S; Jose Blanco-Vidal M; Valiente A; Alba J; Rodriguez-Alvarez R; et al. Excretion and Viability of SARS-CoV-2 in Feces and Its Association with the Clinical Outcome of COVID-19. Sci. Rep 2022, 12, 7397. [PubMed: 35513481]

(75). Lin RD; Steinmetz NF Tobacco Mosaic Virus Delivery of Mitoxantrone for Cancer Therapy. Nanoscale 2018, 10, 16307–16313. [PubMed: 30129956]

(76). Denis J; Majeau N; Acosta-Ramirez E; Savard C; Bedard MC; Simard S; Lecours K; Bolduc M; Pare C; Willems B; et al. Immunogenicity of Papaya Mosaic Virus-like Particles Fused to a Hepatitis C Virus Epitope: Evidence for the Critical Function of Multimerization. Virology 2007, 363, 59–68. [PubMed: 17320136]

(77). Cao J; Guenther RH; Sit TL; Opperman CH; Lommel SA; Willoughby JA Loading and Release Mechanism of Red Clover Necrotic Mosaic Virus Derived Plant Viral Nanoparticles for Drug Delivery of Doxorubicin. Small 2014, 10, 5126–5136. [PubMed: 25098668]

(78). Ward BJ; Makarkov A; Séguin A; Pillet S; Trépanier S; Dhaliwall J; Libman MD; Vesikari T; Landry N Efficacy, Immunogenicity, and Safety of a Plant-Derived, Quadrivalent, Virus-like Particle Influenza Vaccine in Adults (18–64 Years) and Older Adults (≥65 Years): Two Multicentre, Randomised Phase 3 Trials. Lancet 2020, 396, 1491–1503. [PubMed: 33065035]

(79). Pillet S; Couillard J; Trépanier S; Poulin JF; Yassine-Diab B; Guy B; Ward BJ; Landry N Immunogenicity and Safety of a Quadrivalent Plant-Derived Virus like Particle Influenza Vaccine Candidate—Two Randomized Phase II Clinical Trials in 18 to 49 and ≥ 50 Years Old Adults. PLoS One 2019, 14, e0216533. [PubMed: 31166987]

(80). Pillet S; Aubin É; Trépanier S; Poulin JF; Yassine-Diab B; Ter Meulen J; Ward BJ; Landry N Humoral and Cell-Mediated Immune Responses to H5N1 Plant-Made Virus-like Particle Vaccine Are Differentially Impacted by Alum and GLA-SE Adjuvants in a Phase 2 Clinical Trial. npj Vaccines 2018, 3, 3. [PubMed: 29387473]

(81). Landry N; Ward BJ; Trepanier S; Montomoli E; Dargis M; Lapini G; Vezina L-P Preclinical and Clinical Development of Plant-Made Virus-like Particle Vaccine against Avian H5N1 Influenza. PLoS One 2010, 5, e15559. [PubMed: 21203523]

(82). Hager KJ; Pérez Marc G; Gobeil P; Diaz RS; Heizer G; Llapur C; Makarkov AI; Vasconcellos E; Pillet S; Riera F; et al. Efficacy and Safety of a Recombinant Plant-Based Adjuvanted Covid-19 Vaccine. N. Engl J. Med 2022, 386, 2084–2096. [PubMed: 35507508]

(83). Gilca V; Sauvageau C; Panicker G; De Serres G; Ouakki M; Unger ER Immunogenicity and Safety of a Mixed Vaccination Schedule with One Dose of Nonavalent and One Dose of Bivalent HPV Vaccine versus Two Doses of Nonavalent Vaccine – a Randomized Clinical Trial. Vaccine 2018, 36, 7017–7024. [PubMed: 30314913]

(84). Bi D; Apter D; Eriksson T; Hokkanen M; Zima J; Damaso S; Soila M; Dubin G; Lehtinen M; Struyf F Safety of the AS04-Adjuvanted Human Papillomavirus (HPV)-16/18 Vaccine in Adolescents Aged 12–15 Years: End-of-Study Results from a Community-Randomized Study up to 6.5 Years. Hum. Vaccines Immunother 2020, 16, 1392–1403.

(85). Velicer C; Zhu X; Vuocolo S; Liaw KL; Saah A Prevalence and Incidence of HPV Genital Infection in Women. Sex. Transm. Dis 2009, 36, 696–703. [PubMed: 19652630]

(86). Focà A; Liberto MC; Quirino A; Marascio N; Zicca E; Pavia G Gut Inflammation and Immunity: What Is the Role of the Human Gut Virome? Mediators Inflamm 2015, 2015, 1–7.

(87). Scarpellini E; Ianiro G; Attili F; Bassanelli C; De Santis A; Gasbarrini A The Human Gut Microbiota and Virome: Potential Therapeutic Implications. Dig. Liver Dis 2015, 47, 1007–1012. [PubMed: 26257129]

(88). Wellink J Comovirus Isolation and RNA Extraction. Plant Virol. Protoc 1998, 81, 205–209.

(89). Chan SK; Steinmetz NF Isolation of Tobacco Mosaic Virus-Binding Peptides for Biotechnology Applications. ChemBio-Chem 2022, 23, e202200040.

(90). Chan SK; Du P; Ignacio C; Mehta S; Newton IG; Steinmetz NF Biomimetic Virus-Like Particles as Severe Acute Respiratory Syndrome Coronavirus 2 Diagnostic Tools. ACS Nano 2021, 15, 1259–1272. [PubMed: 33237727]

(91). Shukla S; Dickmeis C; Fischer R; Commandeur U; Steinmetz NF Planta Production of Fluorescent Filamentous Plant Virus-Based Nanoparticles. In Virus-Derived Nanoparticles for Advanced Technologies; Wege C, Lomonossoff GP, Eds.; Springer: New York, NY, 2018; pp 61–84.

(92). Ortega-Rivera OA; Shin MD; Chen A; Beiss V; Moreno-Gonzalez MA; Lopez-Ramirez MA; Reynoso M; Wang H; Hurst BL; Wang J; et al. Trivalent Subunit Vaccine Candidates for COVID-19 and Their Delivery Devices.J. Am. Chem. Soc 2021, 143, 14748–14765. [PubMed: 34490778]

(93). Shukla S; Roe AJ; Liu R; Veliz FA; Commandeur U; Wald DN; Steinmetz NF Affinity of Plant Viral Nanoparticle Potato Virus X (PVX) towards Malignant B Cells Enables Cancer Drug Delivery. Biomater. Sci 2020, 8, 3935–3943. [PubMed: 32662788]

(94). Ma Y; Commandeur U; Steinmetz NF Three Alternative Treatment Protocols for the Efficient Inactivation of Potato Virus X. ACS Appl. Bio Mater 2021, 4 (12), 8309–8315.

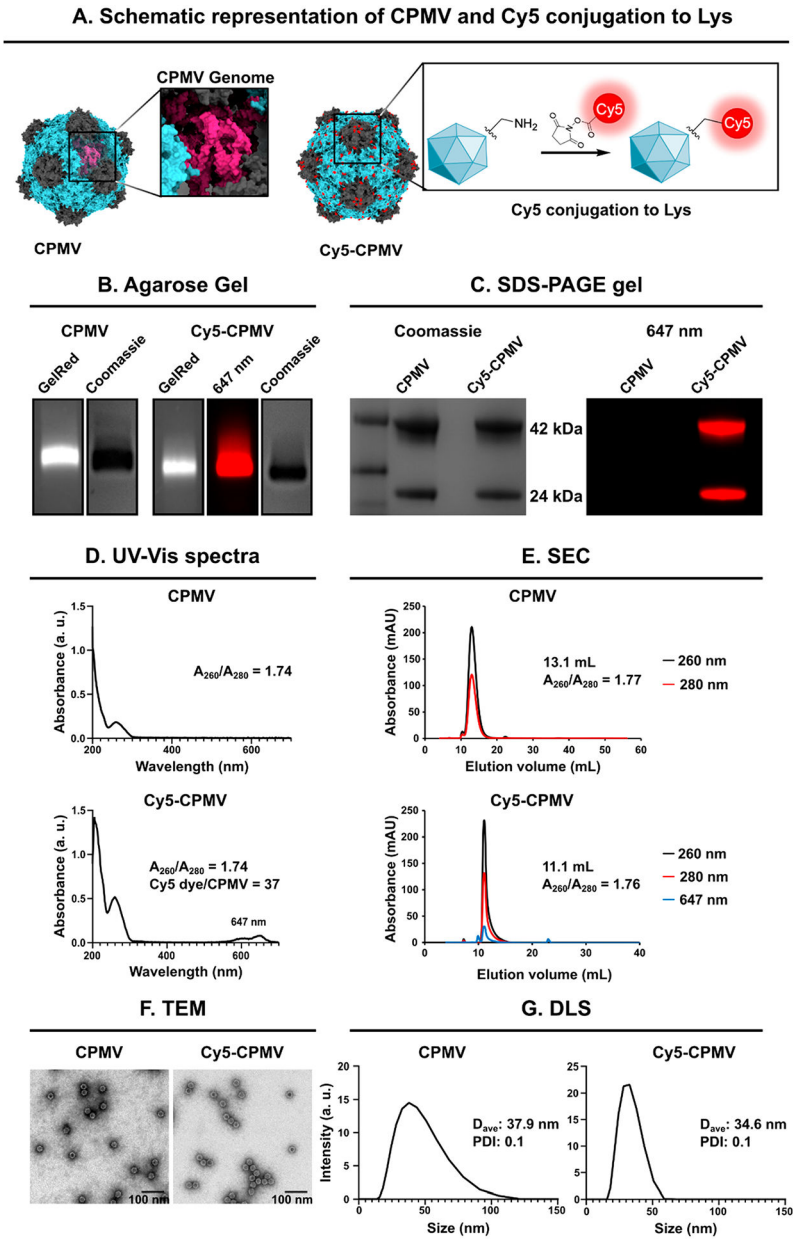

Figure 1.

Characterization and bioconjugation of CPMV and Cy5-CPMV particles. (A) Structure of CPMV and Cy5-CPMV was created on UCSF Chimera X, version 1.2 (2021-05-24) using Protein Data Bank (PDB) entry 1NY7 for CPMV and RNA PDB 4GXY. NHS chemistry was used to conjugate fluorescent dye Sulfo-Cy5 to the CPMV's surface lysine residues (reaction scheme was created using ChemDraw Ultra 7.0). (B) Native agarose gel electrophoresis stained with GelRed nucleic acid stain and Coomassie Brilliant Blue; gels were imaged under UV light and white light. (C) Denaturing 4–12% Nu-PAGE was imaged on a FluorChem R imager, first using the MultiFluor Red channel under 607 nm excitation (fluorescence image) to verify dye conjugation and then stained with GelCode Blue Safe protein stain and visualized under white light (stained image). The small (S, 24 kDa) and

large (L, 42 kDa) coat proteins of CPMV were detected. (D) UV–visible light spectra and 260/280 nm ratio of CPMV and Cy5-CPMV. (E) Particle integrity was determined using size exclusion chromatography and a Superose 6 increase column; the A260/A280 nm ratio is shown and Cy5 is detected at 647 nm. (F) TEM images of negatively stained CPMV and Cy5-CPMV. Scale bars correspond to 100 nm. (G) Dynamic light scattering of CPMV and Cy5-CPMV. Average hydrodynamic diameter (denoted as D in nm) and polydispersity index are shown.

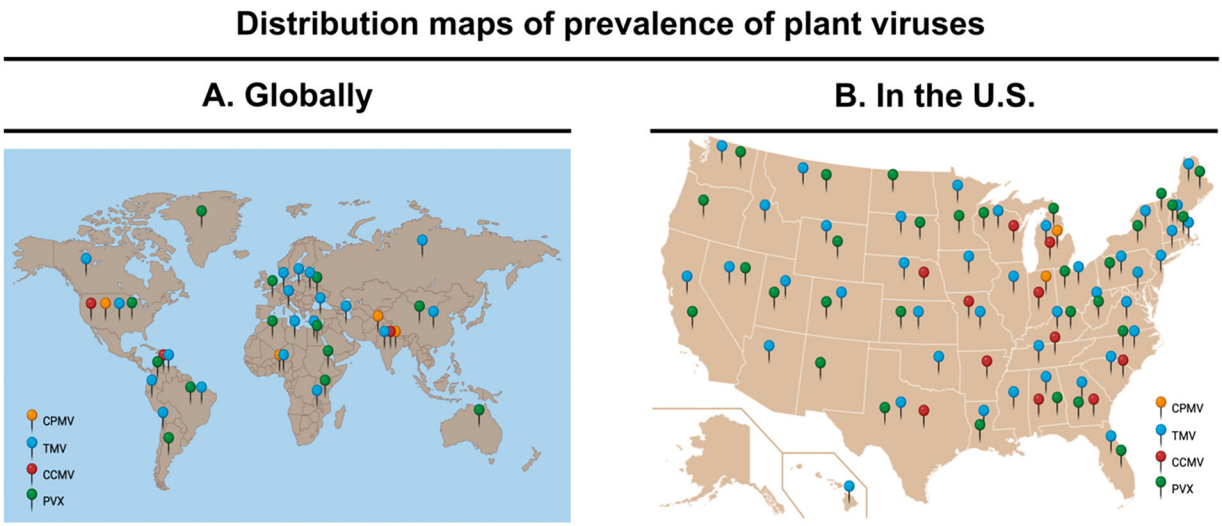

Figure 2.

(A) Overview of the global distribution of plant viruses[56] and (B) widely prevalent plant viruses in the U.S.[57] The figure was created with BioRender.com.

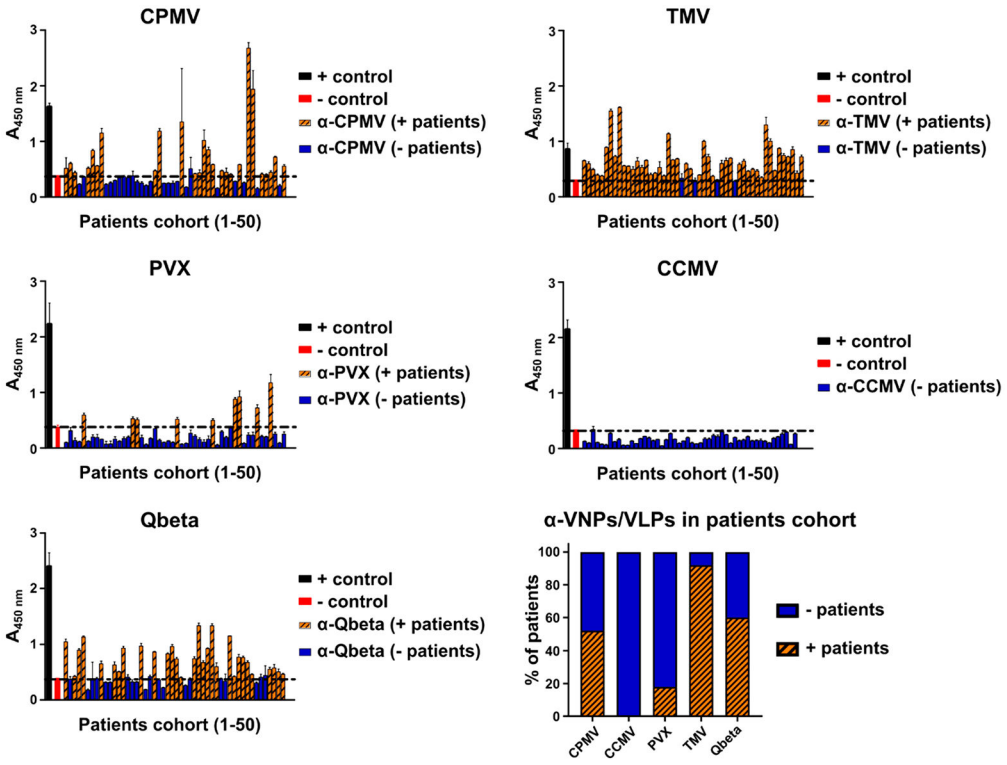

Figure 3.

Detection of antiplant virus antibodies in human plasma using an ELISA-based assay. The presence of anti-VNP/VLP antibodies was evaluated in a 50 patient cohort. Individual ELISA results as well as % positive patients are shown.

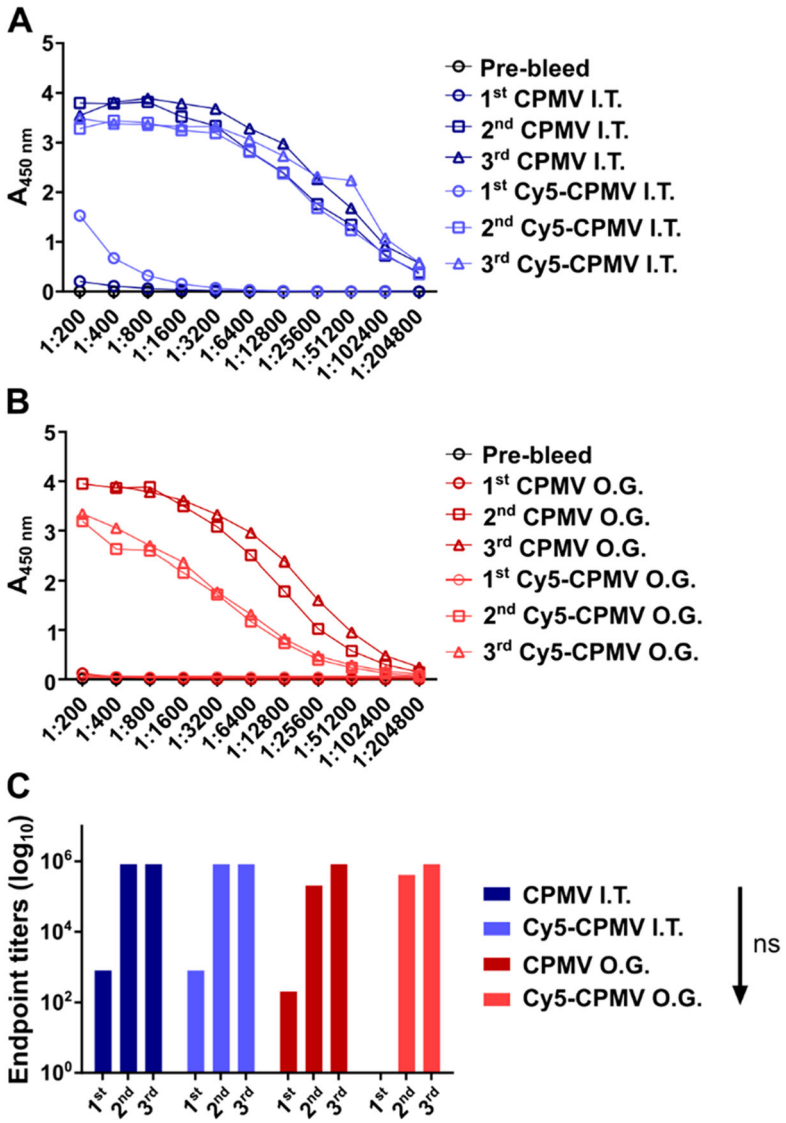

Figure 4.

Immunogenicity of CPMV and Cy5-CPMV after oral gavage (O.G.) or intratumoral (I.T.) administration; mice received three doses (100 μg particles, 5 days apart). Anti-CPMV antibody titers after I.T. (A) and O.G. (B) administration and end point IgG titers (C) as determined by ELISA. Statistical analysis was performed by ordinary one-way ANOVA and Tukey's multiple comparisons test using GraphPad Prism software.

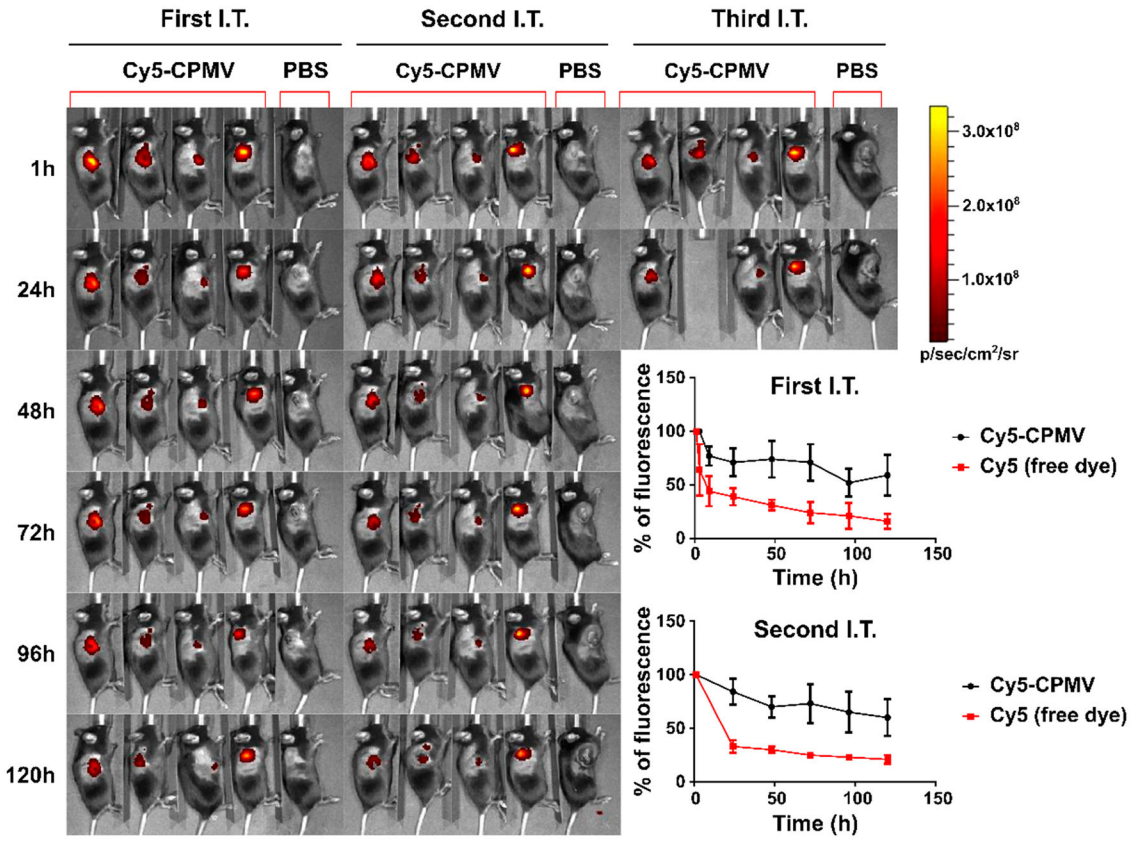

Figure 5.

Biodistribution of Cy5-CPMV after I.T. administration (three times in 5 day intervals) into dermal B16F10 tumors using C57BL/6 mice; imaging was performed daily and up to 24 h after the third I.T. treatment using IVIS. Cy5-CPMV and free Cy5 were compared; while Cy5 is cleared rapidly, Cy5-CPMV persists within the tumor. Inset shows quantification of the signals (average signals and standard deviation) over the 5 day time course after the first and second I.T. administration.

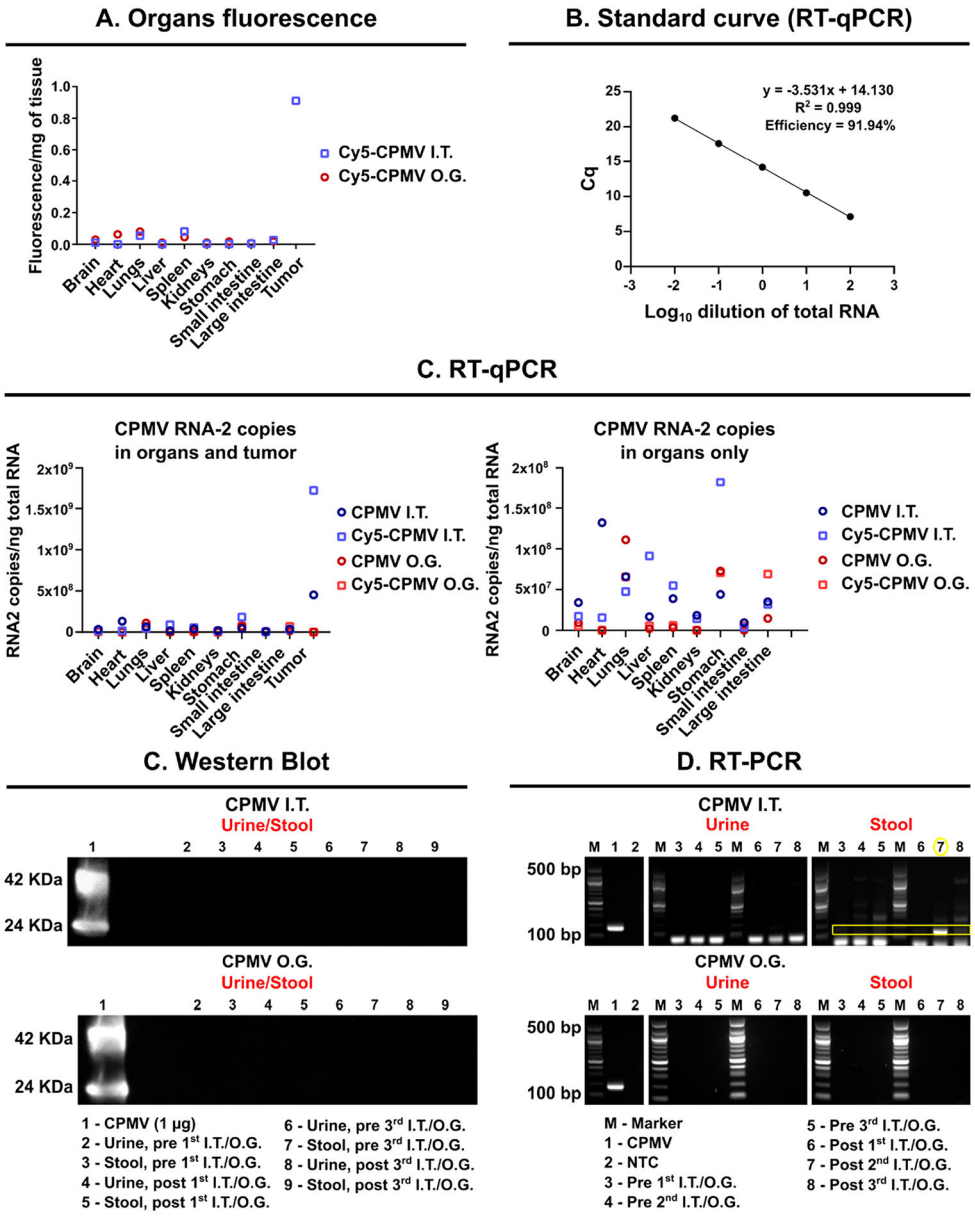

Figure 6.

Biodistribution of CPMV/Cy5-CPMV after I.T. or O.G. administration (three treatments every 5 days) using B16F10 tumor-bearing mice or healthy C57BL/6 mice; tissues were collected 24 h after the final treatment. (A) Fluorescence signals of homogenized organs of animals receiving Cy5-CPMV. (B) RT-qPCR standard curve of CPMV. (C) RT-qPCR of homogenized organs of animals receiving CPMV; data are graphed with and without the tumor. To evaluate possible shedding of CPMV particles, stool and urine samples were collected and analyzed using (D) Western blot and (E) RT-PCR to detect protein or RNA. For RT-PCR, a 100 bp DNA ladder was used as the marker (M).

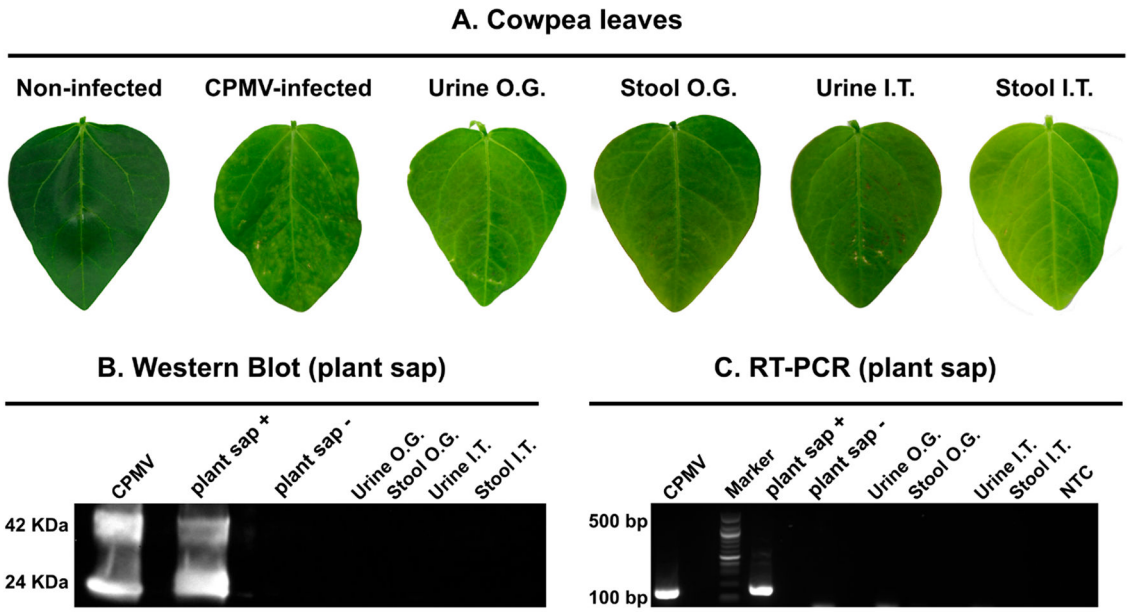

Figure 7.

Analysis of the infectivity of urine and stool collected from mice receiving I.T. or O.G. dosing of CPMV; the natural host *V. unguiculata* (black-eyed pea No. 5) and a mechanical inoculation protocol were used. (A) Photographs of leaves 10 days after mechanical inoculation. (B) Western blot of sap from pulverized leaves probed with a primary rabbit anti-CPMV antibody followed by secondary goat anti-rabbit HRP-conjugated antibody. (C) Total RNA was extracted from leaf sap, and RT-PCR was performed. A 100 bp DNA ladder was used as the marker (M).

Table 1.

Rabbit Anti-VNP/VLP Antibody (Pacific Immunology) Used As Positive Controls on ELISA

VNP/VLP	buffer	rabbit anti-VNP/VLP polyclonal antibody
cowpea mosaic virus (CPMV)	KP 0.1 M, pH 7	PAC 12273/12274
cowpea chlorotic mottle virus (CCMV)	buffer B (0.1 M NaOAc, 1 mM EDTA), pH 4.8	PAC 11777/11778
tobacco mosaic virus (TMV)	KP 10 mM, pH 7	PAC-12267/12268
potato virus X (PVX)	KP 0.1 M, pH 7	PAC 12269/12270